RECENT ADVANCES IN AIRBORNE INSAR FOR 3D APPLICATIONS

Bryan Mercer, Qiaoping Zhang

Intermap Technologies Corp., #1200, 555 - 4th Avenue SW, Calgary, AB, Canada T2P 3E7
{bmercer, qzhang}@intermap.com

Commission I, WG I/2

KEY WORDS: DEM, DSM, DTM, InSAR, Interferometric SAR, Mapping

ABSTRACT:

The objective of this paper is to provide an update on two programs which have been evolving recently that will have significant impact on several geomatics application areas requiring 3D information over extended areas. The first program relates to the creation of nation-wide and continental-scale DEM databases using airborne Interferometric SAR (InSAR) at a level of detail intermediate between that of airborne lidar and space-borne systems. This program is operational and well advanced in its goal. The second program is developmental, and concerns a first-of-its-kind airborne, single-pass L-Band, fully polarimetric InSAR (PolInSAR) system. The primary goal of this research is to determine how well ground elevation can be extracted beneath forest canopy of different types in the absence of temporal decorrelation effects. Some preliminary results are presented here.

1. INTRODUCTION

The use of Digital Elevation Models (DEMs) is widely spread and growing, not only in the traditional mapping world but increasingly in support of new applications that are driven by consumer interests. In this new environment, not only do required levels of detail and implicit accuracy vary according to application, but price and current availability are major considerations for the user, many of whom come from outside the geomatics industry. An additional consideration is that some applications, in order to be effective, transcend local political boundaries and require uniform data-sets across regional, national and even continental scales. Meanwhile the advances of enabling technologies such as GPS, communications bandwidth, storage capacity and processing power have been instrumental in the growth of both numbers and capability of systems for DEM creation including both passive and active systems. Among the active systems, both lidar and Interferometric SAR (InSAR) have become major sources of three-dimensional information.

In particular, airborne InSAR, as demonstrated in the following sections, is contributing to the wide-spread availability of DEMs over continent-sized areas and across national boundaries with properties of accuracy, resolution and price that are intermediate between those of lidar and SRTM. The objective of the first part of this paper is to provide an update on the NEXTMap® programs for creating DEMs of Western Europe and the USA using well-developed operational airborne X-Band InSAR technology. The second part of the paper, by contrast, describes the early phases of a developmental program, the objective of which is to extract bare-earth DEMs from beneath forest canopy using single-pass airborne L-Band Polarimetric InSAR (PolInSAR) techniques.

In the following sections we will first provide a brief background with respect to the InSAR technology, and summarize the specifications and validation of the various DEM and image products created by the STAR-series of airborne InSAR platforms. This will be followed by a discussion of the NEXTMap® concept with an update of the current implementation status and a description of the current capacity of the acquisition and processing elements required to achieve the NEXTMap® goals and schedule. The developmental program will then be addressed, first discussing some aspects of L-Band PolInSAR. A few preliminary results from the recent tests single-pass tests will then be presented.

2. INSAR BACKGROUND

2.1 InSAR Summary

The interferometric process has been widely discussed in the literature, (e.g. Zebkor and Villsenor, 1992; Bamler and Hartl, 1998; Rodriguez and Martin, 1992). The geometry relevant to height extraction, h, is illustrated in Figure 1. If the two antennas, separated by baseline B, receive the back-scattered signal from the same ground pixel, there will be a path-difference δ between the two received wave-fronts. The baseline angle θ_b is obtainable from the aircraft inertial system, the aircraft height is known from differential GPS and the distance from antenna to pixel is the radar slant range. Then it is simple trigonometry to compute the target height h in terms of these quantities as shown in Equations 1-3.

$$\sin(\theta_f - \theta_b) = \delta / B \quad (1)$$

$$\delta / \lambda = \varphi / (2*\pi) + n \quad (2)$$

$$h = H - r_s \cos(\theta_f) \quad (3)$$

The path-difference δ is measured indirectly from the phase difference φ between the received wave fronts (Equation 2). Because the phase difference φ can only be measured between 0 and 2π (modulo 2π), there is an absolute phase ambiguity (n wavelengths) which is normally resolved with the aid of relatively coarse ground control. A "phase unwrapping" technique completes the solution. Thus the extraction of elevation is performed on the "unwrapped" phase. Often the

InSAR is operated in a so-called ping-pong mode which effectively doubles the value of the geometric baseline *B*. These equations become the basis for sensitivity and error analysis (e.g. Rodriguez and Martin, 1992). For single-pass InSAR airborne systems as described in this work, the signals are received almost simultaneously so that errors induced by temporal-decorrelation are not a factor as is the case for satellite systems such as ERS and Radarsat which operate in a repeat-pass mode. Provided the baseline length, position (from DGPS) and attitude (from coupled GPS/inertial) are adequately controlled and/or measured, the dominant noise-like error source arising out of these sensitivity equations is 'phase noise σ_φ' so that the signal-to-noise ratio, which is a function of flying height among other system-related factors, becomes a means of (partly) controlling height error specifications. That is, other parameters being fixed, the height noise will increase as a function of flying height. For example, DEMs created from the STAR-3*i* system, when operated at about 9km altitude, has a height-noise level of about 0.5 m (1 sigma, 5 m sample spacing) at the far edge of the swath. Systematic errors, with reference to STAR-3*i* DEMs, are usually slowly-varying and arise from a variety of sources but are limited through calibration, operational and processing procedures

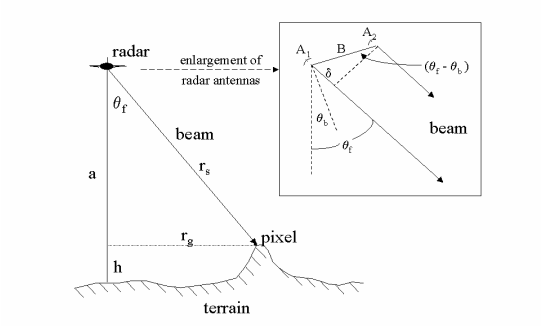

Figure 1. Schematic of Airborne IFSAR Geometry.

2.2 Current Intermap Airborne InSAR Systems

In order to meet the schedule requirements of its NEXTMap® program (Section 3) and other demands, Intermap has recently developed three additional operational airborne InSAR systems (Figure 2) to supplement the acquisition capability of the STAR-3*i*® system. STAR-3*i*, is an X-band, HH polarization InSAR flown on a Learjet 36 (Tennant and Coyne, 1999). In the last few years, all of the software and most of the hardware has been replaced in order to improve product quality and efficiency of operation. The new systems are based on a common architecture and are flown in 2 King Air and 1 Lear Jet platforms respectively. The systems are described in somewhat greater detail in Chapter 6 of (Maune, 2007). The addition of these systems has greatly improved scheduling flexibility and capacity.

2.3 Product Specifications

The core InSAR products available from Intermap's online store include an Ortho-rectified Radar Image (ORI), a Digital Surface Model (DSM) and the bare earth Digital Terrain Model (DTM). X-band images are at 1.25-m resolution with similar horizontal accuracy. DSM and DTM are posted at 5m spacing. The elevation products are available in three standard vertical accuracy specifications as illustrated in Table 1 below. It is worth noting that all four of the STAR family of sensors are able to achieve these product specifications despite the nuance of individual system design or platform specifics. Apart from these core specifications, other accuracies and image/DEM resolutions can be supported to meet specific requirements. Optical/radar merged products are now also becoming available as exemplified in Section 3.

Figure 2. Clockwise from upper left: STAR-3*i*, STAR-4, STAR-6 and STAR-5.

Product Type	DSM		DTM	
	RMSE	Spacing	RMSE	Spacing
I	0.5	5	0.5	5
II	1	5	1	5
III	3	10	-	-

Table 1. Intermap Core Product specifications for InSAR DSMs and DTMs. All units are meters. RMSE refers to vertical accuracy and is with respect to terrain that is moderately sloped, bare (DSM) and unobstructed. DTM specifications apply to areas for which the forest or other above ground cover is 'patchy' to a maximum scale of about 100 meters. Details of these specifications may be found at www.intermap.com.

2.4 Operational Components

The operational flow consists of four major stages: (1) planning and acquisition, (2) interferometric processing, (3) editing and finishing, and (4) Independent Quality Control, after which the data are delivered to the data base repository. The operational concept has evolved to accommodate the requirements imposed by the current NEXTMap® goals as well as custom projects. The NEXTMap® Europe and USA objectives alone require the data acquisition for an area incorporating 10.2 million km^2 by the end of 2008. All aspects of production are managed with rigorous QC checks throughout and within the framework of ISO9000 certification.

3. NATIONAL MAPPING PROGRAMS: NEXTMAP

NEXTMap® is the term used by Intermap to describe its InSAR-based national and regional mapping programs. Specifically the concept is to make DSM, DTM and ORI products generally available in a seamless fashion over national and trans-national regions where multiple applications and markets may benefit. By retaining ownership and licensing the data to multiple users, the cost is shared, making it feasible for public and private organizations to have access to these data

sets in whole or part. The Type II specification for the DSM creates a level of detail (1m RMSE vertical accuracy, 5 meter sample spacing) intermediate between lidar or photogrammetrically-produced products on the one hand, and SRTM or SPOT5 products on the other. The associated ORI carries a resolution of 1.25 m and horizontal accuracy less than 2m RMSE.

NEXTMap Britain was implemented in 2002/2003 (England and Wales) and subsequently extended to include Scotland (for a description, see Mercer, 2004). On the basis of the success of that project, as well as lessons learned, the decision was made to proceed with a NEXTMapUSA project with the current goal of 2009 completion. As of May, 2008 about 65% of the 8 million km^2 in the USA (lower 48 states) had been acquired and over 1/4 of these data had been interferometrically processed, edited, QC'd and delivered to the data base repository. An example is shown in Figure 3 of the DSM of the State of California.

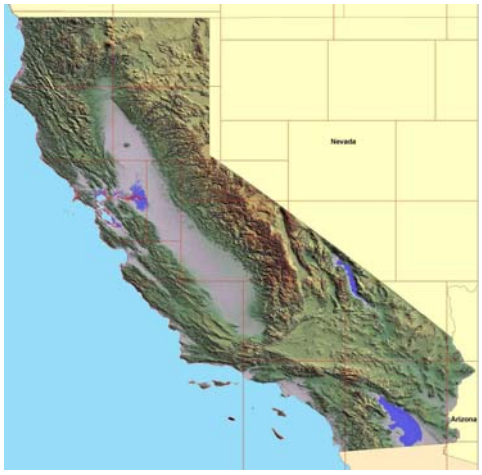

Figure 3. NEXTMAP USA Example - California DSM, validated vertical accuracy (1430 check points) 0.76 m RMSE

NextMAP Europe, a major trans-national program, was initiated in 2006 and currently includes eighteen countries in a single block comprising 2.2 million km^2 combined area. The data acquisition phase is now complete and as the various stages of the processing flow are completed, the database repository will be progressively populated with early 2009 scheduled for overall completion.

Examples from two application areas which should benefit from the availability of NEXTMap coverage are shown here. In Figure 4 a flood risk application is exemplified, while in Figure 5 a visualization example is presented. In both cases the DSM is draped by a high resolution colour air photo. Because of the availability of the 1.25 m ORI it is possible to easily ortho-rectify the air photos using rational functions procedures (or similar), making the co-registration of air-photo to DSM relatively simple. The flood risk application involves 3rd-party models for which the DSM product is an important input component. The visualization example relates to many applications and markets ranging from recreation to automotive safety. In this instance it is a scene extracted from a fly-through (Eye-Tour).

4. SINGLE-PASS L-BAND POLINSAR SYSTEM

4.1 Introduction

As noted earlier, X-Band and C-Band InSAR, which are the major sources of DEM data from airborne and satellite platforms respectively, are usually measuring the elevation of the upper part of the canopy, not the ground below. At longer wavelengths (L-Band and P-Band), attenuation is less but can still be appreciable (Bessette and Ayasli, 2001). The received backscatter signal comprises both canopy and ground components and the interferometric phase difference receives contributions from both sources, thus implying that the apparent phase center will be somewhere above the ground. Elegant methods have been created (e.g. Treuhaft and Siqueira, 2000; Papathanassiou and Cloude, 2001) to separate the ground and canopy contributions at L-Band using combined polarimetric and interferometric (PolInSAR) data. While considerable success has been demonstrated using PolInSAR, most of the validation effort relates to the extraction of tree height rather than DEM information (Zhang, *et. al.*, 2008, and references therein). Moreover, all L-Band PolInSAR efforts to date have used repeat-pass data. This results in two significant problems: (1) temporal decorrelation, and (2) uncompensated residual sensor motions. The former degrades both tree height and DTM extraction accuracy while the latter generates systematic errors of the DEM in the along-track direction. Recent attempts (Reigber, *et. al.*, 2006) to apply repeat-pass E-SAR data acquired during the INDREX-II campaign illustrate some of the problems.

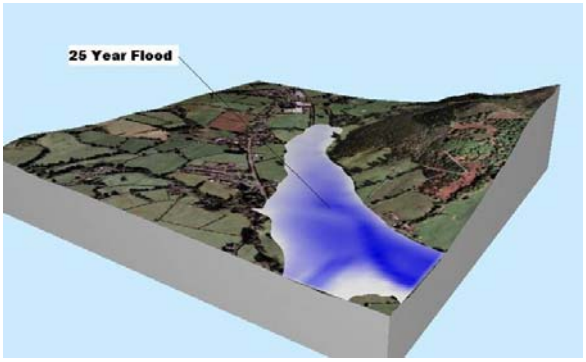

Figure 4. Example from NEXTMap Britain flood risk application

Figure 5. Example from NEXTMap USA - California scene extracted from a fly-through near San Francisco

In order to determine what bare-earth DEM accuracies are achievable under various types of forest and terrain condition, a fully polarimetric, single-pass interferometric L-Band system has been assembled, and tests have recently commenced. It has the virtue that as a single-pass system, temporal decorrelation and residual motion effects should not impact the results. In the following sections we will summarize the system design, describe the processing methodology, and provide some early results from our preliminary data.

4.1.1 Design Philosophy: This system is intended to answer the question posed above: what are the achievable bare-earth DEM accuracies achievable under a range of forest and topography conditions? The concept behind the design of this system is that the experimental platform should be relatively inexpensive, consistent with the experiment needs and be deployable in as short a period as possible. Thus there is no attempt to satisfy more operational considerations. In particular, we allow ourselves the luxury of flying at a relatively low altitude, at the expense of a narrow swath. The results of the tests, if positive, would be used to develop a follow-on strategy including, potentially, a more appropriate design for operational use.

4.1.2 System Description: The L-Band system is an adaptation of the TopoSAR system described in (Maune, 2007). The TopoSAR system previously supported simultaneous X-Band (HH, single-pass InSAR) and P-Band (quad-pol, repeat-pass InSAR). For purposes of this work, the TopoSAR digital infra-structure is used to support only the L-Band (22.6 cm wavelength) channels. The antennas, located at the ends of a 3.5 meter rigid baseline, measure (HH,VV,HV,VH) in a pulse-sequential fashion. The design test altitude (1000m) was chosen to match the minimum S/N requirements (given the relatively modest power and antenna gain specifications for the available hardware).

4.2 Ground Extraction Methodology

4.2.1 The PolInSAR Model: We utilize the well-known Random Volume Over Ground (RVoG) Model (Treuhaft and Siqueira, 2000; Papathanassiou and Cloude, 2001) in which the projection of the observed complex coherences onto the unit circle represents the ground phase (Papathanassiou and Cloude, 2001). This is expressed in Equation (4) as

$$\tilde{\gamma}(\vec{w}) = \exp(i\phi_0)\frac{\tilde{\gamma}_V + m(\vec{w})}{1 + m(\vec{w})} \qquad (4)$$

in which ϕ_0 is the phase related to the ground topography, m is the effective ground-to-volume amplitude ratio (accounting for the attenuation through the volume) and $\vec{w}$ represents the observed polarization state. $\tilde{\gamma}_V$ denotes the complex coherence for the volume alone (excluding the ground component), and is a function of the extinction coefficient σ for the random volume, its height h_V and the vertical wavenumber Kz.

The key point of interest for this application is the assumption that m is polarization dependent while $\tilde{\gamma}_V$ is not. In particular, for large m, the straight line intersects the unit circle (Figure 6) and the associated phase at this point relates directly to the desired ground elevation. In the limit of no ground component (m=0), the observed coherence is given by the volume coherence, $\tilde{\gamma}_V$ rotated through ϕ_0. These two limiting situations therefore determine the line geometry as shown in Figure 6.

Two approaches are available to estimate the straight line: in the first, we create a number of $\vec{w}$-dependent coherences based on lexicographic, Pauli and magnitude optimized coherences (Papathanassiou and Cloude, 2001) and find a regression line amongst them. In the second method we use a phase optimization approach (Tabb, *et. al.*, 2002) which traces out the boundary of the coherence region and from which, if well-behaved, an ellipse is formed whose major axis represents the straight line solution. Using simulated data, the ground phase results for the two approaches are similar. However with repeat-pass data differences can be significant. Although it is a secondary objective in this work, the model is also inverted (Papathanassiou and Cloude, 2001) to extract canopy height.

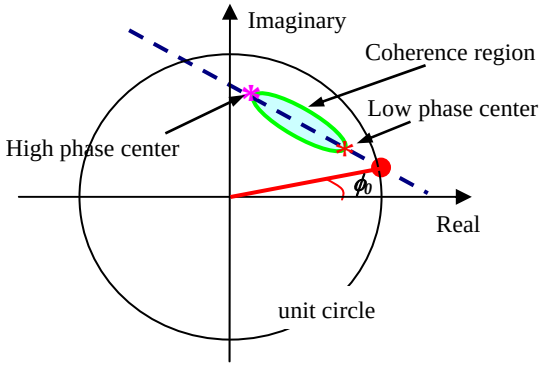

Figure 6. Phase optimization approach for topographic phase estimation: The green ellipse is the estimated coherence region. The straight line (blue dashed) passes through two ends of the coherence region. The ground topographic phase centre is estimated from one of the line-circle intersection points (red circle).

4.2.2 Design Implications: A fundamental parameter of the model is K_z, the vertical wavenumber, defined in Equation (5). On the one hand it determines the sensitivity of the derived height to changes in phase through $h = \phi_0 / K_z$. Secondly it impacts $\tilde{\gamma}_V$ through the relationship $K_v = K_z h_v/2$ and hence the overall coherence observed as well as the line length. From this perspective an optimum K_z can be defined (Hellmann and Cloude, 2004) that is effectively 'tuned' to the canopy height. Given the baseline limitations in this work, an appropriate flying altitude, H is determined such that K_v is optimized for tree heights in the 10-30m region.

$$Kz \approx \frac{4\pi}{\lambda}\frac{B}{H}\frac{\cos\theta}{tg\theta} \qquad (5)$$

4.2.3 Calibration: Both polarimetric and interferometric calibration is required. The polarimetric calibration uses a modified Quegan (Quegan, 1994) approach with trihedrals and forest data allowing for range-dependant imbalance and cross-talk corrections, respectively, to be applied to each antenna.

4.3 Planned Test Program and Current Status

The intent is to acquire data in several areas representing different forest conditions and topography. In all cases, ancillary data are required as part of the validation exercise. Selection of the test sites is based upon the availability and quality of the following data sets:

- Lidar ground data for validation of the PolInSAR-derived bare-earth DEM,
- X-band data from previous STAR-3*i* or TopoSAR campaigns will be used for corroboration of tree height,
- Reports on species, tree heights, stem density, DBH, etc as available from public or private sources

Preliminary tests have occurred, enabling engineering issues to be addressed and mitigated. SNR at the 25db level has been confirmed for VV and HH in bare areas. Polarimetric calibration has led to cross-talk less than -25 db which is deemed adequate. Polarization imbalances have been corrected to the 5%/5 degree level (amplitude/phase).

4.4 Preliminary results

Some preliminary results have been obtained from one of the datasets acquired recently. The test site is in a heavily forested region containing a pattern of alternate forest and clearcut areas. The forest in this area is mainly composed of pine trees with height ranging from 10-25m and with relatively homogeneous growth in the forested patches. Figure 7 shows a ground photo looking towards the forest. The forest in this location is quite dense, with estimated tree heights about 20m on average. A bare-earth DEM was available for truth (30 cm accuracy quoted by Terrapoint, the supplier). Also, an X-Band DSM from the TopoSAR system flown in 2006 (prior to the L-Band configuration change) was available to provide an under-estimated reference of the canopy height.

Figure 7. Ground photo during L-Band data acquisition

The coherence (magnitude) optimization and coherence region algorithms have been applied to the calibrated dataset. The elevation derived from the optimized coherence magnitude follows the terrain quite well on the bare/new growth areas but inside the forest canopy appears to be similar to the X-Band DSM height. The elevation derived from the phase optimization process within the forest patches however, reflects the ground elevation over most of the test area.

In Figure 8 we show the result of merging the two results such as to preserve elevation continuity across the forest boundary. The blue line shows the merged elevation profile representing the terrain while the green line and the red lines are the approximate canopy and bare-earth elevations from X-Band and lidar respectively. The merged L-Band DEM remains within 5 meters of the 'truth' within the 15-20 meter forest. However it fails in the sloped region where canopy heights are reduced. This is possibly because the model is not optimized for trees in this height range. This issue is to be addressed.

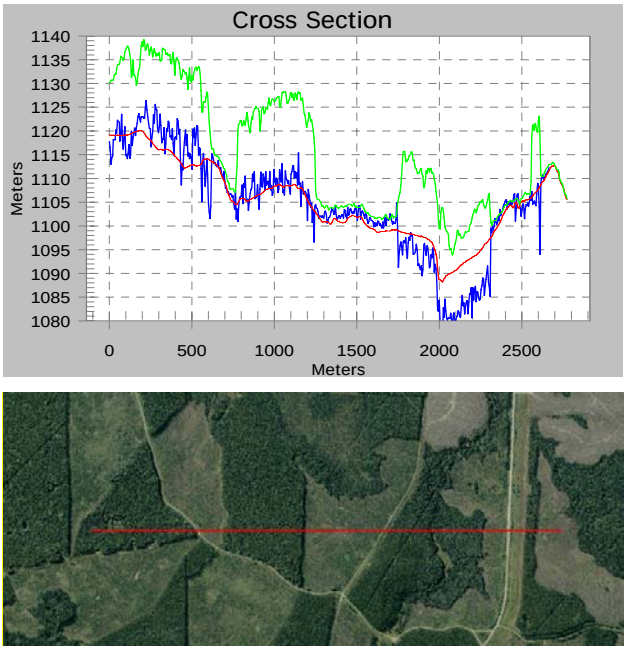

Figure 8. Top: Elevation cross-profile of lidar bald-earth (Red), X-Band DSM (data acquired in April 2006, Green), L-Band ground elevation (blue). Bottom: Location of the profile line is overlaid on a color airphoto.

5. SUMMARY AND CONCLUSIONS

The NEXTMap® program, based upon airborne X-Band HH InSAR, is in the process of creating a 3-dimensional, homogeneous, seamless database including DSM, DTM and ORI products, for eighteen countries of Western Europe and for the USA (excluding Alaska). The DSM is specified at 1 m RMSE vertical accuracy for 5 m sample spacing, while the ORI is specified at 1.25m resolution with better than 2 m RMSE horizontal accuracy. For many applications the combination of detail provided, national and super-national availability and shared pricing through license arrangements should produce an attractive user opportunity. The creation of the product datasets for both areas is well underway and scheduled for completion, in the case of Western Europe, for late 2008 and about 1 year later for the USA. With respect to many market applications such as visualization, flood risk, and auto safety these products should occupy a solid niche, relative to alternative technologies.

The second part of this paper has described a new experimental airborne, single-pass L-Band, fully polarimetric InSAR system, which is currently under test. It has been developed in the context of a particular set of objectives: to provide a test-bed for the extraction of bare-earth DEMs beneath extended forest canopy. PolInSAR techniques are being used to extract the information acquired during a series of test flights in forested areas for which suitable ground truth is available. The overall objective of the program is to determine the accuracy with which bare-earth DEMs can be extracted using PolInSAR methodology in the absence of temporal decorrelation and motion effects. Some preliminary PolInSAR results have been presented to illustrate current status (May, 2008). Further results should be available for presentation at the ISPRS2008 conference.

REFERENCES

Bamler, R. and Hartl, P., 1998. Synthetic aperture radar interferometry, *Inv. Probl.*, Vol. 14, pp. R1–R54, 1998.

Bessette, L.A., Ayasli, S., 2001. Ultra-wideband P-3 and CARABAS II foliage attenuation and backscatter analysis, *Proceedings of the 2001 IEEE Radar Conference*, Atlanta, GA, USA, pp.357 – 362, 2001.

Hellmann, M., Cloude, S.R. 2004. Polarimetric Interferometry and Differential Interferometry, published in RTO-EN-SET-081, 2004.

Maune, D.F., 2007. *Digital Elevation model Technologies and Applications: The DEM Users Manual*, 2nd Edition, ASPRS.

Mercer, B., 2004, DEMs Created from Airborne IFSAR – An Update, *Proceedings of the ISPRS XXth Congress*, July 12-23, Istanbul, Turkey.

Papathanassiou, K.P. and Cloude, S.R., 2001. Single-Baseline Polarimetric SAR Interferometry, *IEEE Transactions on Geoscience and Remote Sensing*, Vol. 39, No.11, pp.2352-2363, 2001.

Quegan, S., 1994. A Unified Algorithm for Phase and Cross-Talk Calibration of Polarimetric Data – Theory and Observations, *IEEE Transactions on Geoscience and Remote Sensing*, Vol. 32, No.1, pp.89-99, 1994.

Reigber, A., Mercer, B., Prats, P., Maduck, J., Kahr, E., 2006. Spectral Diversity Methods Applied to DEM Generation from Repeat-Pass P-Band InSAR, *Proceedings of EUSAR 2006*, May 16-18, 2006, Dresden, Germany.

Rodriguez, E., and Martin, J.M., 1992. Theory and design of interferometric synthetic aperture radars. *IEE Proceedings-F, Vol. 139, No. 2, pp. 147-159.*

Tabb, M., Orrey, J., Flynn, T., Carande, R., 2002. Phase Diversity: A Decomposition for Vegetation Parameter estimation using Polarimetric SAR Interferometry, *Proceedings of EUSAR 2002*, pp. 721-724.

Tennant, J.K. and Coyne, T., 1999. STAR-3*i* interferometric synthetic aperture radar (INSAR): some lessons learned on the road to commercialization. In: *Proceedings of the 4th International Airborne Remote Sensing Conference and Exhibition/21st Canadian Symposium on Remote Sensing*, June 21-24, Ottawa, Ontario, Canada.

Treuhaft, R.N., and Siqueira, P.R., 2000. The vertical structure of vegetated land surfaces from interferometric and polarimetric radar. *Radio Science*, Vol. 35, No. 1, pp. 141-177, 2000.

Zebker, H.A. and Villasenor, J., 1992. Decorrelation in Interferometric Radar Echoes, *IEEE Transactions on Geoscience and Remote Sensing*, Vol. 30: Number 5, pp 950-959.

Zhang, Q., Mercer, B., and Cloude, S.R., 2008. Forest height estimation from INDREX-II L-band polarimetric InSAR data, *Proceedings of the ISPRS XXIth Congress*, July 3-11, 2008, Beijing: China.

ACKNOWLEDGEMENTS

The authors would like to acknowledge their many colleagues at Intermap who have made the NEXTMap program a reality, Dr. Shane Cloude who has provided significant help and insight regarding theoretical and practical PolInSAR issues, and Alberta Ingenuity Fund for partial financial support. We also thank Terrapoint Canada Inc. for providing the lidar ground truth data.